

Isorhamnetin Ameliorates *Aspergillus fumigatus* Keratitis by Reducing Fungal Load, Inhibiting Pattern-Recognition Receptors and Inflammatory Cytokines

Xue Tian,¹ Xudong Peng,¹ Jing Lin,¹ Yingxue Zhang,² Lu Zhan,¹ Jiao Yin,¹ Ranran Zhang,¹ and Guiqiu Zhao¹

¹Department of Ophthalmology, The Affiliated Hospital of Qingdao University, Qingdao, Shandong Province, China

²Department of Biochemistry, Microbiology and Immunology, Wayne State University School of Medicine, Detroit, Michigan, United States

Correspondence: Guiqiu Zhao, Department of Ophthalmology, The Affiliated Hospital of Qingdao University, NO. 16 Jiangsu Road, Qingdao, Shandong Province, 26600, China;

zhaoguiqiu_good@126.com.

Xudong Peng, Department of Ophthalmology, The Affiliated Hospital of Qingdao University, No. 16 Jiangsu Road, Qingdao, Shandong Province, 26600, China; doctordpxd@126.com.

XT and XP are joint first authors.

Received: October 14, 2020

Accepted: February 16, 2021

Published: March 30, 2021

Citation: Tian X, Peng X, Lin J, et al. Isorhamnetin ameliorates *Aspergillus fumigatus* keratitis by reducing fungal load, inhibiting pattern-recognition receptors and inflammatory cytokines. *Invest Ophthalmol Vis Sci.* 2021;62(3):38. <https://doi.org/10.1167/iov.62.3.38>

PURPOSE. Isorhamnetin is a natural flavonoid with both antimicrobial and anti-inflammatory properties, but its effect on fungal keratitis (FK) remains unknown. The current study aims to investigate the antifungal and anti-inflammatory effects of isorhamnetin against mouse *Aspergillus fumigatus* keratitis.

METHODS. In vitro, the lowest effective concentration of isorhamnetin was assessed by minimum inhibitory concentration and cytotoxicity tests in human corneal epithelial cells (HCECs) and RAW264.7 cells. The antifungal property was investigated by scanning electron microscopy and propidium iodide uptake test. The anti-inflammatory effect of isorhamnetin in HCECs and RAW264.7 cells was observed by quantitative real-time polymerase chain reaction (qRT-PCR). In the eyes of mice with *A. fumigatus* keratitis, FK severity was evaluated using clinical score, plate counting, histological staining and periodic acid Schiff staining. In vivo, the anti-inflammatory effect of isorhamnetin was examined by immunofluorescence staining, myeloperoxidase assay, Western blot, enzyme-linked immunosorbent assay, and qRT-PCR.

RESULTS. In HCECs and RAW264.7 cells, isorhamnetin significantly inhibited *A. fumigatus* conidia growth and hyphae viability at 80 µg/mL without affecting cell viability. In vitro, isorhamnetin altered *A. fumigatus* hyphal morphology and membrane integrity. In *A. fumigatus* keratitis mouse model, isorhamnetin treatment alleviated the severity of FK by reducing corneal fungal load and inhibiting neutrophil recruitment. In addition, the mRNA and protein expression levels of TLR-2, TLR-4, Dectin-1, IL-1β, and tumor necrosis factor-α were significantly decreased in isorhamnetin-treated groups in vivo and in vitro.

CONCLUSIONS. Isorhamnetin improves the prognosis of *A. fumigatus* keratitis in mice by inhibiting the growth of *A. fumigatus*, reducing the recruitment of neutrophils and down-regulating inflammatory factors.

Keywords: isorhamnetin, *A. fumigatus*, fungal keratitis, anti-inflammatory, antifungal

Fungal keratitis (FK) is a serious ocular disease that can cause vision impairment and even blindness. In developing countries, the overall trend of corneal ulcer morbidity is still increasing in recent years, with reports of up to 60% of cases attributable to fungal infection.¹⁻³ However, at present, the commonly used antifungal agents (e.g., natamycin and voriconazole) for FK are not effective against the clinically prevalent fungal pathogens, including *Fusarium* and *Aspergillus* because of drug resistance,⁴ and the corneal intrastromal injection may cause stroma tissue damage without improving FK prognosis.⁵ Therefore it is of significance to develop more effective antifungal treatments.

Isorhamnetin (3,5,7-trihydroxy-2-[4-hydroxy-3-methoxyphenyl] chromen-4-one) is an important natural flavonoid extracted from the fruits of *Hippophae rhamnoides* L.

and the leaves of *Ginkgo biloba* L.^{6,7} To date, numerous investigations revealed that isorhamnetin has extensive pharmacological activities and biological effects, such as anti-inflammation,⁸ antimicrobial,^{9,10} cardiovascular and cerebrovascular protection,^{11,12} antitumor,¹³ and antioxidation.¹⁴⁻¹⁶ For example, isorhamnetin could increase pathogen cell membrane permeability by generating oxidative species in a dose-dependent manner,¹⁷ thus exhibiting antifungal activity on *Aspergillus niger*, *Fusarium sporotrichum*, and *Candida albicans* in vitro.¹⁸ But whether isorhamnetin effects the growth of *Aspergillus fumigatus*, one of the most common fungal pathogens for FK, remains unknown. On the other hand, isorhamnetin has been shown as an anti-inflammatory substance in many diseases, such as osteoarthritis,¹⁹ periodontitis,²⁰ and acute lung injury.⁸

Isorhamnetin exerts protective effects on lipopolysaccharide (LPS)-induced acute lung injury in mice by inhibiting the expression of cyclooxygenase-2.¹⁵ It also suppresses LPS-mediated inflammatory response in BV2 microglia through inhibiting the nuclear factor (NF)- κ B signaling pathway, downregulating Toll-like receptor 4 (TLR4) and eliminating reactive oxygen species accumulation.²¹ In addition, the anti-tuberculosis property of isorhamnetin has been reported in murine model via repressing the expression of proinflammatory mediators including tumor necrosis factor (TNF)- α , interleukin (IL)-1 β , IL-6, and IL-12.⁹ These findings indicate the anti-inflammatory potential of isorhamnetin in FK treatment.

In FK, corneal inflammation and its related complications, such as corneal edema, ulcer, and hypertrophic scarring, are important causes of impaired vision and blindness.²² In the pathogenesis of FK, pattern recognition receptors (PRRs) expressed on innate immune cells recognize and bind to pathogen-related molecular patterns in fungal cell walls, which in turn activates the signaling cascade composed of neutrophils, macrophages, proinflammatory cytokines, and chemokines, mediating the eradication of the pathogens.^{23,24} However, excessive inflammatory response-induced accumulation of large numbers of immune cells and cytotoxic substances in the infected site may cause delayed wound healing or tissue damage, resulting in poor prognosis.^{25,26} For example, in cystic fibrosis zebrafish, as a result of the enhanced and sustained accumulation of neutrophils at tail fin wounds, the healing area was reduced by 30% compared with normal control, and the reduced wound healing was significantly improved by genetic ablation of neutrophil.²⁷ Therefore antifungal therapy combined with immunomodulatory therapy is considered to be the most effective strategy to improve the clinical outcome of *Aspergillus*-related infection.

In the current study, we investigated the antifungal and anti-inflammatory effects of isorhamnetin on FK in vitro and in vivo. Our data demonstrated that isorhamnetin alleviated the severity of *A. fumigatus* keratitis, inhibited the growth of *A. fumigatus*, and ameliorated corneal inflammation by repressing neutrophil infiltration and the expression of inflammatory factors, providing a promising alternative treatment for FK.

MATERIALS AND METHODS

Preparation of Isorhamnetin Solution

Isorhamnetin powder 320 μ g purchased from MedChem Express (Shanghai, China) was dissolved in 5 μ L of dimethyl sulfoxide (DMSO, Solarbio, Beijing, China), and further diluted to 1 mL of required solvent to obtain 320 μ g/mL of isorhamnetin solution (0.5% DMSO).

Preparation of *A. fumigatus*

A. fumigatus strain 3.0772 (China General Microbiological Culture Collection Center, Beijing, China) conidia were acquired by washing *A. fumigatus* malt agar slant with phosphate-buffered saline solution (PBS) containing 0.1% Tween 20. The conidia suspension was prepared by repeated resuspension and centrifugation (12,000 rpm, five minutes) for minimum inhibitory concentration (MIC) experiment. *A. fumigatus* hyphae was cultivated in a medium containing 4% glucose and 1% mycophenolate mofetil. The hyphae was

crushed into pieces of 20 to 40 μ m, washed with sterile PBS, and centrifuged at 4000g/min for 40 minutes. After discarding the supernatant, the obtained activated fungi were used in animal experiments, and inactivated fungi treated with 70% alcohol were used in in vitro cell experiments. PBS and Dulbecco's modified Eagle medium (DMEM; Gibco, San Diego, CA, USA) were used to dilute *A. fumigatus* to 3×10^8 CFU/mL.²⁸

MIC for *A. fumigatus* Conidia

Isorhamnetin MIC for *A. fumigatus* conidia was assayed by a standardized microdilution method in the 96-well plate. 320 μ g/mL of isorhamnetin in sabouraud medium (0.5% DMSO) was diluted to 7 different concentrations by two-fold gradient dilution, then transferred into third to ninth column wells (100 μ L per well). The first column was the blank control, the second column was incubated with sabouraud medium with 0.5% DMSO. Finally, 5 μ L prepared conidia suspension (4×10^6 CFU/mL) was added into the 96-well plate. The plates were incubated at 37°C for 48 hours. The isorhamnetin MIC₉₀ was determined spectrophotometrically and was recognized as the lowest concentration that could inhibit 90% growth of *A. fumigatus*.²⁹

MIC for *A. fumigatus* Hyphae

XTT (2,3-bis-(2-methoxy-4-nitro-5-sulphenyl)-(2H)-tetrazolium-5-carboxanilide) assay was used to test the impact of isorhamnetin against *A. fumigatus* hyphae. Conidia suspension (4×10^6 CFU/mL) was incubated in 12-well plates (1 mL per well) at 37°C for 24 hours to form hyphae, then 5 μ L DMSO was added with 0, 5, 10, 20, 40, 80, 160 and 320 μ g isorhamnetin per well and incubated for 24 hours. After harvesting and washing with sterile PBS, resuspended hyphae was transferred into the 96-well plate. After incubating with 20 μ L XTT Assay Kit (Abcam, Shanghai, China) per well for 2 hours, *A. fumigatus* hyphae MIC was determined spectrophotometrically at 450 nm.

Cell Viability Assay (CCK-8)

Human corneal epithelial cells (HCECs; provided by Laboratory, University of Xiamen, Fujian, China) (3×10^4 /mL) were cultured in growth medium that contained 1:1 DMEM/Hams F12 supplemented with 5% fetal bovine serum, 10 ng/mL human epidermal growth factor, 5 mg/mL insulin, and 50 mg/mL penicillin and streptomycin. Mouse macrophages (RAW264.7) were purchased from the Cell Bank of the Chinese Academy of Sciences typical culture preservation Committee (Shanghai, China) and maintained in DMEM (high glucose) and 10% fetal bovine serum. Cells were cultured in the 96-well plates in an incubator (37°C, 5% CO₂) until 80% confluency. After PBS rinsing, the original liquid in the well was removed, and 100 μ L of different concentrations of isorhamnetin/F12 medium (5, 10, 20, 40, 80, 160, and 320 μ g/mL) was added to each well. DMSO 0.5% was added to the culture medium of solvent control group, and 100 μ L of F12 medium was added as the blank control. The plates were incubated for 24 hours in the incubator. 10 μ L of the Cell Counting Kit-8 (Solarbio, Beijing, China) was added to each well, and the plate was incubated at 37°C for two hours. The absorbance was measured at 450 nm with a microplate reader.³⁰

Scanning Electron Microscopy (SEM)

A. fumigatus conidia (4×10^6 CFU/mL) was cultured in 12-well plates (1 mL per well) at 37°C for 24 hours to form hyphae. Then, the hyphae were washed, centrifuged (12,000 rpm, 10 minutes), and transferred to a new 12-well plate, followed by incubation with 0.5% DMSO or 80 µg/mL isorhamnetin for 24 hours at 37°C. After PBS rinsing was performed three times, the hyphae were collected, fixed by 2.5% glutaraldehyde and treated according to the method described by Zhang et al.³¹ Images were photographed by SEM (JSM-840; JOEL Company, Japan) at magnification $\times 2000$ and $\times 5000$.

Propidium Iodide (PI) Uptake Testing

PI uptake testing was used to determine the fungal membrane integrity on isorhamnetin treatment. The conidia suspension of *A. fumigatus* (4×10^6 CFU/mL) was seeded into 6-well plates and incubated at 37°C for 24 hours to form hyphae. Then the hyphae were washed, centrifuged (12,000 rpm, 10 minutes), and transferred to a new 12-well plate, followed by incubation with 0.5% DMSO or isorhamnetin (40, 80, 160 µg/mL) for 24 hours at 37°C. After rinsing with PBS, 1 mL 50 µg/mL PI solution was added to each well for 15 minutes' incubation at room temperature in the dark. Images were captured with a fluorescence microscope (magnification $\times 200$; Zeiss Axio Vert; Zeiss, Oberkochen, Germany) under green excitation light.

HCECs and RAW264.7 Culture and *A. fumigatus* Stimulation

HCECs and RAW264.7 cells were cultured as described above. For *A. fumigatus* stimulation, cells were seeded in 12-well plates and stimulated with or without inactivated *A. fumigatus* hyphae for 1 hour, followed by isorhamnetin (80 µg/mL) or DMSO (0.5%) treatment for eight hours. The control groups were treated with 80 µg/mL isorhamnetin and 0.5% DMSO without hyphae stimulation. Total RNA were collected for quantitative real-time polymerase chain reaction (RT-qPCR).^{32,33}

Animal Models of FK

Female eight-week-old C57BL/6 mice were purchased from Sibeifu Laboratory Animal Co. (Beijing, China). All animals were treated in accordance with the ARVO Statement for the Use of Animals in Ophthalmic and Vision Research. Mice were anesthetized using 8% chloral hydrate and placed beneath a stereoscopic microscope (magnification $\times 40$), and central corneal epithelium (2 mm diameter range) of the right eye was removed. *A. fumigatus* 5 µL (3×10^8 CFU/mL) was applied to the ocular surface topically. Then the ocular surface was covered with a soft contact lens, and eyelids were sutured for 24 hours to promote the formation of corneal ulcer.

Experimental eyes were treated with 5 µL of isorhamnetin (80 µg/mL) topically, whereas conditional control eyes were treated with DMSO (0.125%). Isorhamnetin treatment began at 24 hours after infection (p.i.) at one to five days, four times per day. Based on the observation under a slit lamp at 1, 3, and 5 days p.i. the severity of keratitis was evaluated by clinical score that sums the three aspects of cornea, including opacity density, opacity area, and surface regularity, each

of which has a grade of 0 to 4. Meanwhile the severity of keratitis was divided into normal (0), mild (1–5), moderate (6–9), and severe (10–12). Mice corneas were removed entirely at the indicated times after treatments and prepared for qRT-PCR, Western blot, enzyme-linked immunosorbent assay (ELISA), myeloperoxidase (MPO) assay, plate count, respectively. Whole eyes were harvested for Immunofluorescence staining (IFS) and hematoxylin and eosin staining (H&E staining).³⁴

Total RNA Extraction, Reverse Transcription, and qRT-PCR

Total RNA of corneas from HCECs and RAWs was extracted using the RNAiso Plus kit (Takara, Dalian, China), and cDNA was obtained by reverse transcription of total RNA using the HiScript III RT SuperMix for qRT-PCR (Vazyme Biotech, Nanjing, China). Finally, qRT-PCR was performed by Eppendorf Mastercycler and SYBR green. The β -actin was used as internal reference.³⁵ The sequences of the oligonucleotide primers are as follows (Tables 1 and 2).

Plate Count

The corneal homogenate was diluted with PBS, spread on the agar plate, and then incubated at 37°C for 48 hours. The viable fungi on the treated cornea ($n = 3$ /group/time) were reflected by taking pictures and counting the colonies.²⁹

MPO Assay

To determine the activity of polymorphonuclear neutrophils, corneas were harvested at 3 days p.i. ($n = 5$ /group/time) and processed according to the instructions of MPO kit (Nanjing Chengjian Institute of Bioengineering, Jiangsu, China). The absorbance at 460 nm was measured by spectrophotometry at 37°C. The slope of the straight line is related to MPO unit/gram cornea.

ELISA

According to the manufacturer's instructions (Elabscience, Wuhan, China), corneas of C57BL/6 mice ($n = 6$ /group/time) at 3 and 5 days p.i. were homogenized in 500 µL PBS containing 0.1% Tween 20 and protease inhibitor (Solarbio) and centrifuged for 10 minutes at 5000g for ELISA analysis. IL-1 β and TNF- α protein expression levels were detected for each sample in duplicate.

Western Blot

The total protein was extracted from corneas by homogenization in radioimmunoprecipitation assay (Solarbio) lysis buffer containing phosphatase inhibitor cocktail and phenylmethanesulfonyl fluoride (Solarbio). Total protein was run on sodium dodecyl sulphate-polyacrylamide gel (GenScript) electrophoresis and transferred to polyvinylidene fluoride membrane (Millipore, Burlington, MA, USA). After blocked with blocking buffer, the membrane was incubated overnight with the primary antibody of the target protein. Primary antibodies against the following proteins were used: Dectin-1 (ABclonal, Wuhan, China), TLR-2 (Affinity, Cincinnati, OH, USA) and TLR-4 (Elabscience, Wuhan, China). After rinsing with PBST for three times, membranes

TABLE 1. Nucleotide Sequence of Mouse Primers Used for RT-PCR

Gene	Nucleotide Sequence	Primer	Gen Bank
β -actin	5'-GATTACTGCTCTGGCTCCTAGC-3'	F	NM_007393.3
	5'-GACTCATCGTACTCCTGCTTGC-3'	R	
TLR-2	5'-CTCCTGAAGCTGTGCGTTAC-3'	F	NM_011905.3
	5'-TACTTTACCCAGCTCGCTCACTAC-3'	R	
TLR-4	5'-CCTGACACCAGGAAGCTTGAA-3'	F	NM_021297.3
	5'-TCTGATCCATGCATTGGTAGGT-3'	R	
Dectin-1	5'-GACCCAAGCTACTTCCTC-3'	F	NM_020008.3
	5'-GCAGCACCTTTGTCATACT-3'	R	
IL-1 β	5'-CGCAGCAGCACATCAACAAGAGC-3'	F	NM_008361.4
	5'-TGTCCTCATCCTGGAAGGTCCACG-3'	R	
TNF- α	5'-ACCCTCACACTCAGATCATCTT-3'	F	NM_013693.2
	5'-GGTTGCTTTGAGATCCATGC-3'	R	

TABLE 2. Nucleotide Sequence of Human Primers Used for RT-PCR

Gene	Nucleotide Sequence	Primer	Gen Bank
β -actin	5'-GCTCCTCTGAGCGCAAG-3'	F	NM_001101.3
	5'-CATCTGCTGGAAGGTGACA-3'	R	
TLR-2	5'-TGCTGTGCTCTGTTCCTGCT-3'	F	NM_001318796.2
	5'-TTCCTGGGCTTCCTTTTGG-3'	R	
TLR-4	5'-CCATTTCAGCTCTGCCTTAC-3'	F	NM_003266.4
	5'-ACAACAATCACCTTTCGGCTTT-3'	R	
Dectin-1	5'-CGACTCTCAAAGCAATACCAGGA-3'	F	NM_197947.3
	5'-GTACCCAGGACCACAGTATCAC-3'	R	
IL-1 β	5'-ATGCACCTGTACGATCACTGA-3'	F	NM_000576.2
	5'-ACAAAGGACATGGAGAACC-3'	R	
TNF- α	5'-TGCTTGTTCCTCAGCCTCTT-3'	F	NM_000594.4
	5'-CAGAGGGCTGATTAGAGAGAGGT-3'	R	

were incubated with the corresponding secondary antibodies (Elabscience) at 37°C for one hour. The blots were tested with chemiluminescence (ECL; Thermo Fisher Scientific, Waltham, MA, USA).³⁶

Periodic Acid Schiff (PAS) Staining

Eyeballs of C57BL/6 mice at 3 days p.i. (n = 3/group/time) were harvested, embedded and frozen in optimal cutting temperature, then sectioned by 8 μ m under cryostat. Sections were stained with glycogen PAS staining kit (Leagene, Beijing, China) and treated with periodate oxidant for 10 minutes, Schiff reagent for 20 minutes, and hematoxylin for two minutes. Each slice was photographed under an optical microscope (magnification \times 400).

H&E Staining

Eyeballs of C57BL/6 mice (n = 3/group/time) were harvested at 3 days p.i. and fixed with 4% paraformaldehyde at 4°C for three days. After the lenses were removed, eyeballs were embedded using paraffin and then sectioned into 8 μ m under cryostat. Slices were treated by conventional H&E staining method and photographed under an optical microscope (magnification \times 400).³⁷

IFS

IFS was performed in conformity with the method described previously.³⁵ The mouse eyeballs (n = 3/group/time) at 3 days p.i. were removed, embedded, and frozen in optimal cutting temperature. Corneal slices at a thickness of 8 μ m

were obtained under cryostat, then fixed in acetone at 4°C and blocked with goat serum (1:100; Solarbio). Monoclonal rat antimouse neutrophil marker (1:100; Santa Cruz Biotechnology Company, Santa Cruz, CA, USA) was used to incubate with the slices, followed by fluorescein isothiocyanate (FITC) conjugated goat anti-rotavirus secondary antibody (1:200; Electronic science). The nuclei were stained with 4',6'-diamidino-2-phenylindole (DAPI) (Solarbio). Images were taken by fluorescence microscope (Zeiss Axio Vert; magnification \times 400).

Statistical Analyses

GraphPad Prism (American GraphPad Prism software) and ImageJ2x (German company, Rawak software) were used as analysis software. The difference of clinical score between two groups was tested by the Mann-Whitney U test. MIC, plate count, ELISA, MPO test, qRT-PCR, and Western blot were analyzed by unpaired two-tailed Student's *t*-tests. One-way analysis of variance with post hoc analysis was used for CCK-8 test and fungal viability assay. *P* < 0.05 indicates significant difference. The experimental data are presented in the form of mean \pm SEM.

RESULTS

Evaluation of Isorhamnetin Antifungal Activity and Host Cell Cytotoxicity

MIC and CCK-8 tests were conducted to screen the effective fungistatic concentration and cytotoxicity of isorhamnetin, respectively. Conidia MIC test showed isorhamnetin

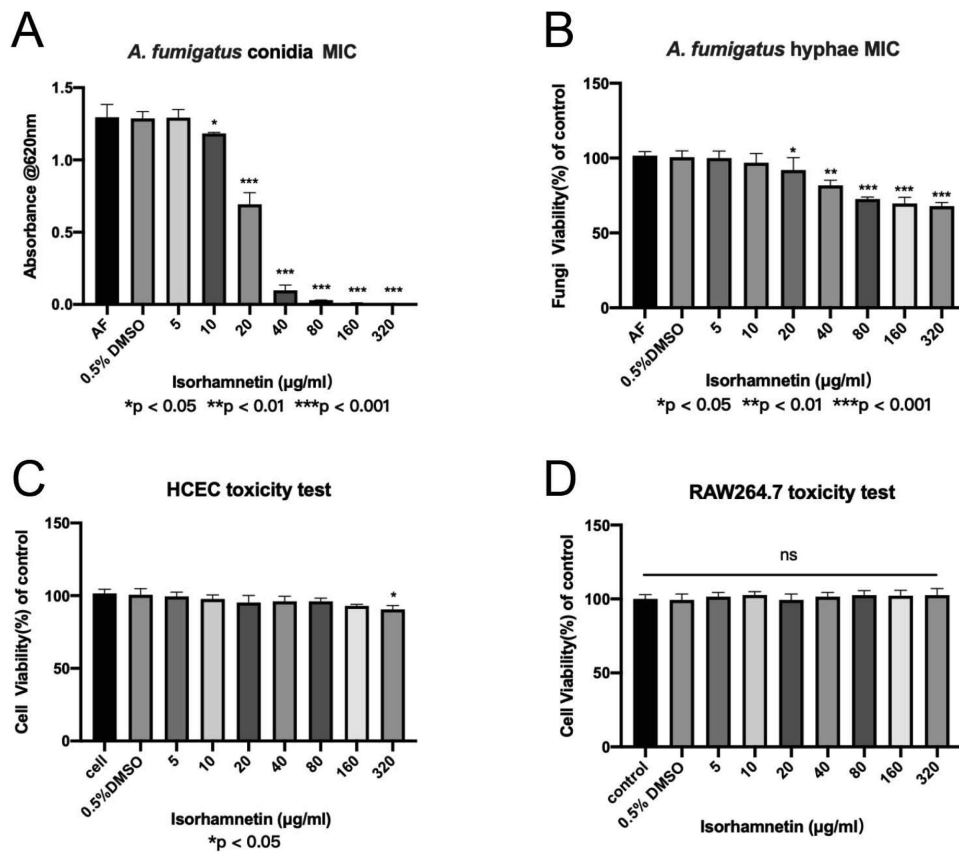


FIGURE 1. Isorhamnetin antifungal activity and host cell cytotoxicity. *A. fumigatus* conidia were cultured with 0.5% DMSO and isorhamnetin at different concentrations (5, 10, 20, 40, 80, 160, and 320 µg/mL) for 48 hours (MIC₉₀ = 80 µg/mL) (A). Isorhamnetin showed antifungal effect at 20 µg/mL and obviously inhibited hyphae viability at 80 µg/mL (B). HCECs and RAW264.7 cells were cultured with isorhamnetin at different concentrations for 24 hours. Cell viability of HCECs (C) and RAW264.7 (D) at different concentrations (0, 5, 10, 20, 40, 80, 160, and 320 µg/mL) of isorhamnetin. All data were mean ± SEM. MIC was analyzed by an unpaired, two-tailed Student's *t*-test, and CCK-8 and fungal viability assay were tested by one-way analysis of variance with post hoc analysis.

started to inhibit the growth of *A. fumigatus* at 10 µg/mL and prevented 90% *A. fumigatus* growth (MIC₉₀) at 80 µg/mL (Fig. 1A). Hyphae MIC showed isorhamnetin started to suppress the viability of hyphae at 20 µg/mL and obviously inhibited hyphae viability at 80 µg/mL (Fig. 1B). CCK-8 was used to test the cell viability of HCECs and RAW264.7 cells at different concentrations of isorhamnetin and 0.5% DMSO. Cells were cultured at a concentration of 5 to 320 µg/mL for 24 hours, and no obvious cytotoxic effect was observed in HCECs (≤ 160 µg/mL) (Fig. 1C) and RAW cells (≤ 320 µg/mL) (Fig. 1D). Thus isorhamnetin with the concentration of 80 µg/mL was considered an effective antifungal concentration and applied to the following in vitro and in vivo experiments.

Isorhamnetin Alters *A. fumigatus* Hyphal Morphology and Membrane Integrity

The effects of isorhamnetin on *A. fumigatus* morphology and membrane integrity were observed by SEM and PI uptake testing. Hyphae treated with 0.5% DMSO showed an intact morphological structure characterized by smooth surface and rounded mycelia (Figs. 2A, 2B), whereas

isorhamnetin (80 µg/mL)-treated hyphae were thinned, swollen, twisted, and knotted (Figs. 2C, 2D). Additionally, PI uptake assay was performed in *A. fumigatus* hyphae incubated with 0.5% DMSO or isorhamnetin (40, 80 and 160 µg/mL) for 24 hours. Nucleic acids exposed from damaged or compromised membranes were stained by PI, a red-fluorescent counterstain, revealing the enhanced fluorescence at the higher concentrations of isorhamnetin (Figs. 2E–2H), which indicated that isorhamnetin affected the permeability of fungal membrane in a dose-dependent manner.

Isorhamnetin Treatment Alleviates the Severity of *A. fumigatus* Keratitis in Mice

The effect of isorhamnetin on FK was recorded from the first day of the treatment. Compared to the DMSO group, the corneas of the isorhamnetin group were more transparent, had smaller ulcers, and did not perforate (Fig. 3A). The clinical score of isorhamnetin treated group was significantly lower than that of DMSO group at 3 and 5 days p.i., although there was no obvious difference among the groups at 1 day p.i. (Fig. 3B). PAS staining of corneal tissue sections showed that isorhamnetin observably reduced fungal hyphal load and alleviated corneal edema on the third day after

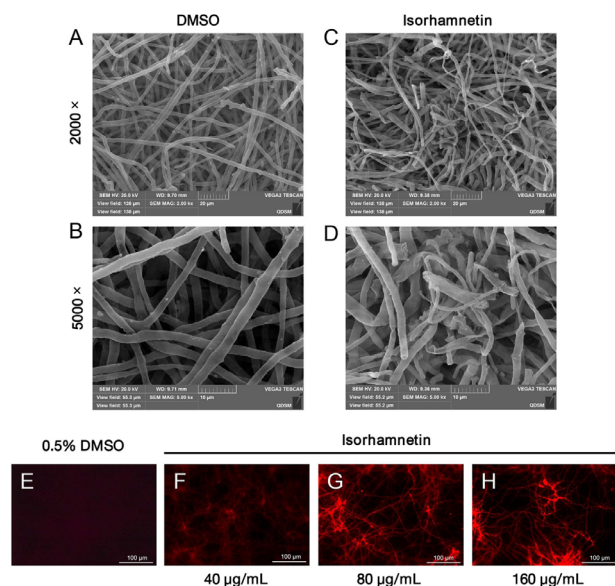


FIGURE 2. Isorhamnetin alters *A. fumigatus* hyphal morphology and membrane integrity. Representative SEM images of *A. fumigatus* hyphae treated by 0.5% DMSO, magnification $\times 2000$ (A) and $\times 5000$ (B), and 80 $\mu\text{g}/\text{mL}$ isorhamnetin, magnification $\times 2000$ (C) and $\times 5000$ (D) for 24 hours. Representative fluorescence images of PI uptake test showed *A. fumigatus* hyphae treated by 0.5% DMSO (E) and isorhamnetin at 40 $\mu\text{g}/\text{mL}$ (F), 80 $\mu\text{g}/\text{mL}$ (G), and 160 $\mu\text{g}/\text{mL}$ (H) for 24 hours (magnification $\times 200$; scale bar: 100 μm).

infection (Figs. 3F, 3G). Plate counting experiment showed that the number of viable fungus in corneas of isorhamnetin group was significantly less than DMSO group on the 5th day after infection (Figs. 3C–3E). These results indicate that isorhamnetin treatment alleviates the severity of *A. fumigatus* keratitis and reduces the fungal load in corneas of C57BL/6 mice.

Isorhamnetin Reduced Neutrophil Infiltration in Mice *A. fumigatus* Keratitis

IFS, MPO assay, and H&E staining were performed to detect the level of neutrophil infiltration in mice with *A. fumigatus* keratitis at 3 days p.i. Compared with the DMSO control group, the number of neutrophils in isorhamnetin treated group was significantly decreased (Figs. 4A, 4B), which is supported by MPO activity assay that neutrophil activity was significantly reduced by isorhamnetin treatment (Fig. 4C). Moreover, H&E staining of corneal tissue sections showed that isorhamnetin significantly reduced inflammatory cell infiltration on the third day after infection (Figs. 4D, 4E). These data suggested that isorhamnetin treatment inhibited the neutrophil infiltration in the *A. fumigatus* keratitis mouse model.

Isorhamnetin Plays an Anti-Inflammatory Role in HCECs and RAW264.7 Cells

We next detected the anti-inflammatory effect of isorhamnetin in both HCECs and RAW264.7 cells. After eight hours of *A. fumigatus* stimulation, the expression levels of PRRs such as TLR-2 (Figs. 5A, 5F), TLR-4 (Figs. 5B, 5G), Dectin-1 (Figs. 5C, 5H), and inflammatory factors including TNF- α (Figs. 5D, 5I) and IL-1 β (Figs. 5E, 5J) were increased in both

cells, whereas isorhamnetin significantly inhibited the intensive trend of inflammatory response (Figs. 5A–5J).

Isorhamnetin Plays an Anti-Inflammatory Role in *A. fumigatus* Keratitis Mouse Model

To evaluate the role of isorhamnetin in the inflammatory response in mice with FK, mRNA and protein expressions of different PRRs and inflammatory factors were detected at 1, 3, and 5 days p.i. *A. fumigatus* induction of TLR-2, TLR-4 and Dectin-1 was significantly inhibited by isorhamnetin in mRNA level at 1, 3, 5 days p.i. (Figs. 6A–6C) and protein level at 3 days p.i. (Figs. 6D–6I). In addition, the mRNA levels of TNF- α and IL-1 β were significantly repressed in isorhamnetin treated groups compared with DMSO control at 1, 3, and 5 days p.i. (Figs. 6J, 6K). ELISA revealed that the protein expression levels of proinflammatory factors TNF- α and IL-1 β were markedly prevented by isorhamnetin at 3 and 5 days p.i. (Figs. 6L, 6M). Neither isorhamnetin nor DMSO induced cytokine expression in uninfected mice.

DISCUSSION

FK is usually a refractory and challenging ophthalmic disease worldwide³⁸ because of the lack of effective antifungal drugs and the uncontrollable excessive inflammatory response, resulting in a corneal perforation rate five to six times higher than bacterial keratitis.^{39,40} Therefore it is necessary to find more effective treatments that display both antifungal and anti-inflammatory effects. In the current study, we investigated the function of isorhamnetin in FK in vitro (HCECs and macrophages) and in *A. fumigatus* keratitis mouse model.

Isorhamnetin is an important active component from *Hippophae rhamnoides L.*, which is a traditional Chinese medicinal plant used as an anti-cough expectorant for pneumonia and detoxifying prescription for viral enteritis.^{10,41} Studies have shown the antifungal property of isorhamnetin,⁴² and it is probably through disrupting fungal cytoplasmic membrane permeability, or acting as a nonionic surfactant that disrupts the function of native membrane-associated proteins, resulting in cell lysis.^{43,44} However, whether isorhamnetin plays antifungal role in *A. fumigatus* keratitis and its toxicity to the cornea are still unknown. Our study revealed that isorhamnetin inhibited the proliferation of *A. fumigatus* in a dose-dependent manner, and isorhamnetin with a concentration of 80 $\mu\text{g}/\text{mL}$ could inhibit the germination of *A. fumigatus* conidia by 90%, directly affecting hyphae growth. The *A. fumigatus* morphology was further investigated by SEM and PI uptake testing. Isorhamnetin markedly altered the normal morphology and membrane integrity of *A. fumigatus* hyphae, making the surface become twisted and deformed. In addition, cell viability of HCECs and RAW264.7 cells was not affected when isorhamnetin concentration was lower than 160 $\mu\text{g}/\text{mL}$. Thus an isorhamnetin concentration at 80 $\mu\text{g}/\text{mL}$ was selected as the effective antifungal concentration and used to the following in vivo and in vitro experiments.

In mice with *A. fumigatus* keratitis, isorhamnetin significantly alleviated the severity and shortened the course of FK. Moreover, plate counting experiments showed that the viable colonies of cornea in the 80 $\mu\text{g}/\text{mL}$ isorhamnetin-treated group were significantly less than those in control group, which is consistent with PAS staining that

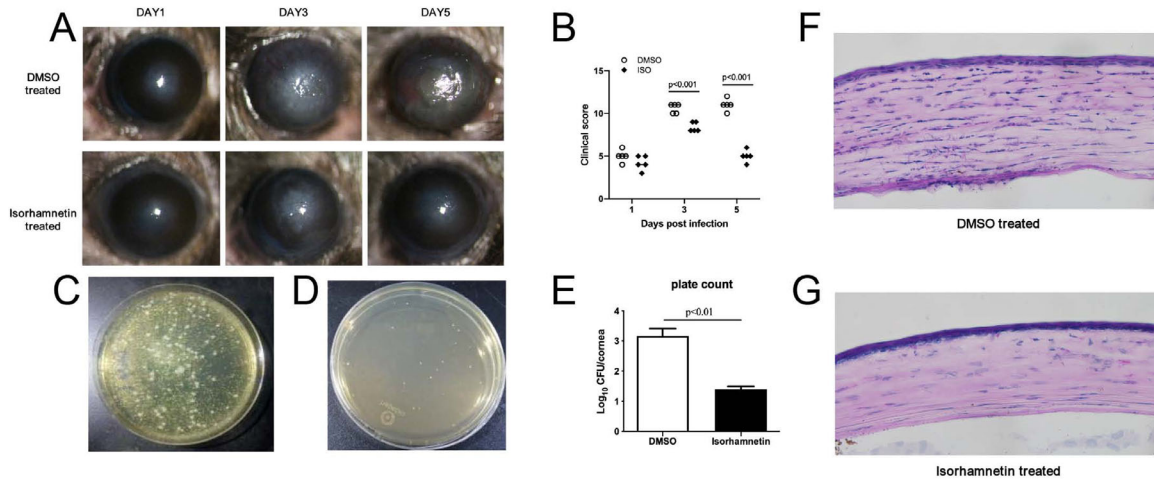


FIGURE 3. FK severity after *A. fumigatus* infection followed by DMSO or isorhamnetin treatment. Representative slit lamp photographs of DMSO or isorhamnetin treated *A. fumigatus* keratitis mice at days 1, 3, and 5 (A). Clinical scores of DMSO or isorhamnetin treated mice cornea (n = 5 mice/group) (B). Representative plates of DMSO (C) or isorhamnetin (D) treated *A. fumigatus*-infected mouse cornea at five days p.i., and quantitative diagram (E). PAS staining of corneal tissue sections (magnification $\times 400$) of DMSO (F) or isorhamnetin (G) treated *A. fumigatus* keratitis mice at three days p.i. (n = 3 mice/group). Clinical scores were analyzed using a nonparametric Mann-Whitney U test. Horizontal lines indicate the median values. Plate count results were analyzed by an unpaired, two-tailed Student's *t*-test.

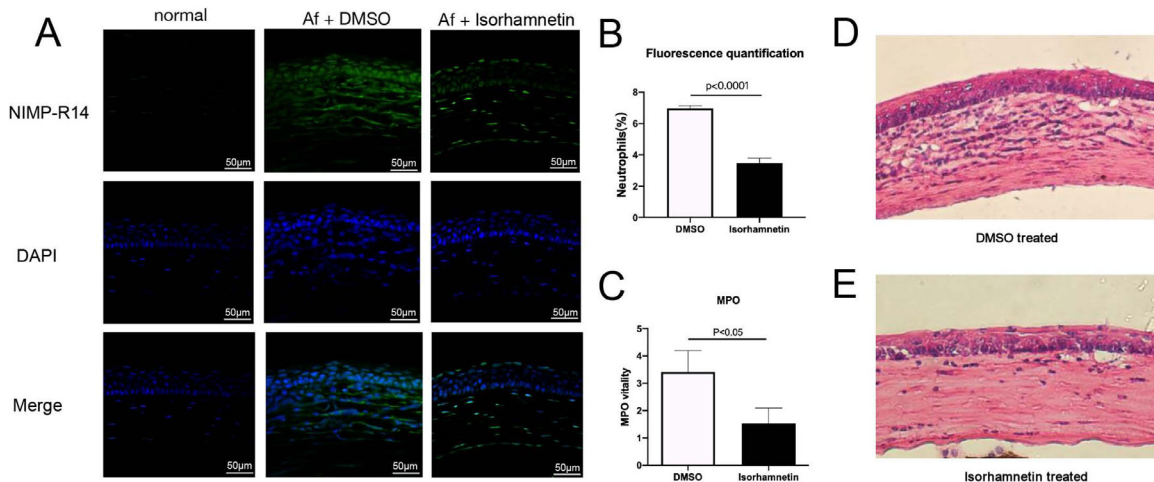


FIGURE 4. Effects of isorhamnetin on neutrophil infiltration in *A. fumigatus* keratitis mouse model. Mice with FK treated with isorhamnetin (80 $\mu\text{g}/\text{mL}$) or 0.5% DMSO, and stained with NIMP-R14-FITC (neutrophils, green) and DAPI (nucleus, blue) (n = 3 mice/group). Representative IFS images of mice corneas (magnification $\times 400$) (A) and quantitative analysis (B). MPO activity in mice with FK treated by isorhamnetin (80 $\mu\text{g}/\text{mL}$) or 0.5% DMSO (n = 5 mice/group) (C). H&E staining of corneal tissue sections (magnification $\times 400$) of DMSO (D) or isorhamnetin (E) treated *A. fumigatus* keratitis mice at day 3 (n = 3 mice/group). All data were mean \pm SEM and analyzed by an unpaired, two-tailed Student's *t*-test.

isorhamnetin obviously decreased the hyphae load in the infected sites. Thus we considered that isorhamnetin could improve infectious corneal ulcer by limiting the growth of *A. fumigatus*. It is the first time the antifungal effect of isorhamnetin is confirmed in FK mice.

Furthermore, we also found that isorhamnetin attenuated inflammatory response by inhibiting neutrophil recruitment in *A. fumigatus* infected corneas. When the cornea is infected by fungi, chemokines released from limbal vessels to infected sites attract numbers of neutrophils that release large amounts of lysosomal enzymes to decompose fungi, thus limiting the invasive fungi from causing further damage to the cornea.^{45–47} However, neutrophils also secrete a large

number of toxic substances and oxygen free radicals, resulting in continuous inflammation reaction that may destroy corneal structure and cause undesirable tissue damage and visual impairment.⁴⁸ Thus the overrecruited neutrophils may lead to poor prognosis of FK because of high production of proinflammatory factors, cytokines, and oxidative stress. In our study, IFS and MPO assays showed that isorhamnetin significantly inhibited neutrophil infiltration to the epithelium and stroma of cornea at 3 days p.i., suggesting the anti-inflammatory potential of isorhamnetin in FK. Similarly, Ren et al.⁴¹ demonstrated that LPS/cigarette smoke exposure-induced elevated cell numbers of neutrophils and macrophages in bronchoalveolar fluid, inflammatory cell

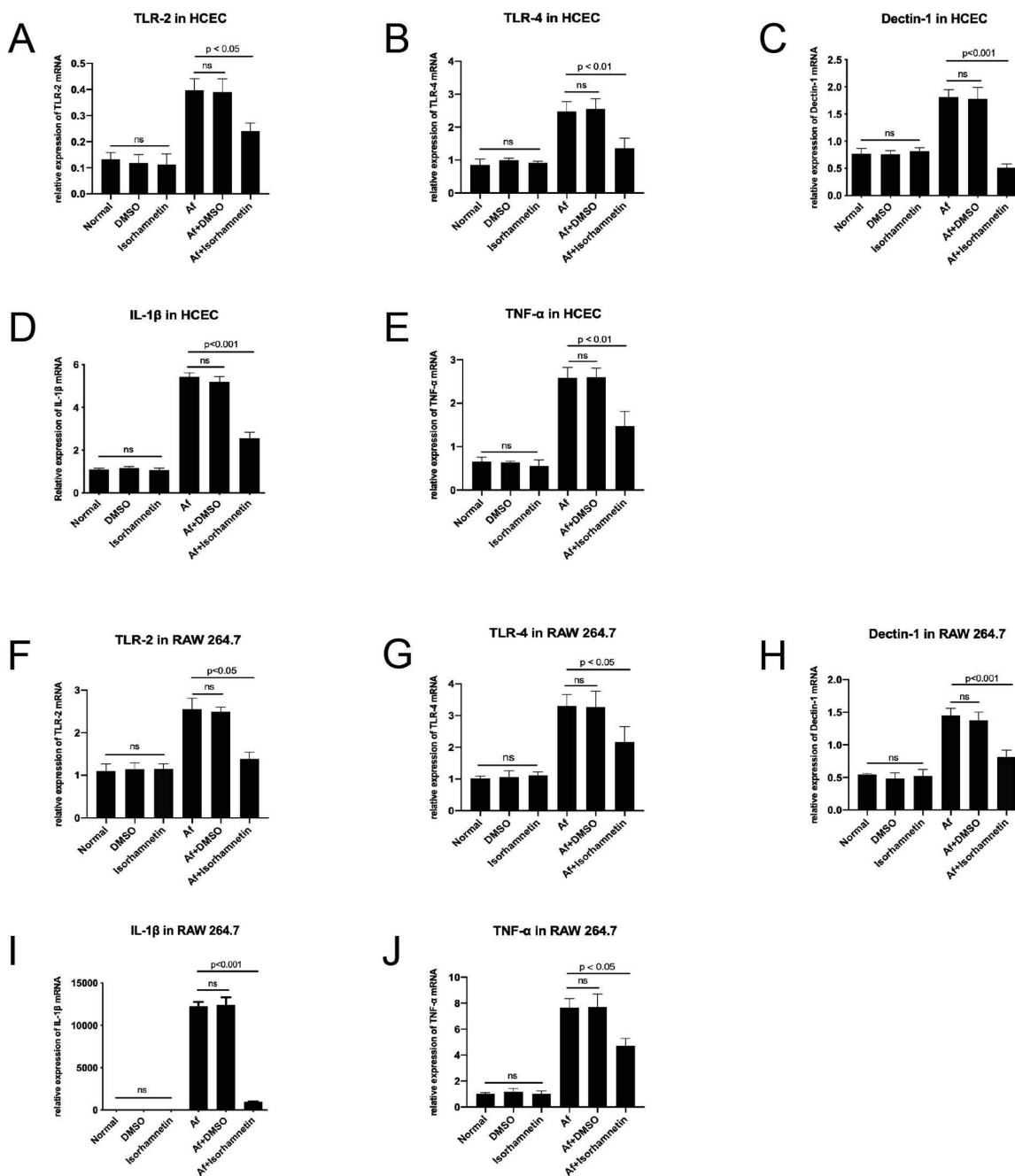


FIGURE 5. Effects of isorhamnetin on the inflammatory response in HCECs and RAW264.7 cells. After stimulating the cells with *A. fumigatus* (60 μ L, 3×10^8 CFU/mL) for two hours, the cells were cultured with isorhamnetin (80 μ g/mL) or 0.5% DMSO for eight hours, and only *A. fumigatus* was added to the culture medium of positive control group. The negative control groups were set as uninfected cells treated with or without isorhamnetin and DMSO. The qRT-PCR was used to detect the mRNA level of each group. Compared with the control groups, isorhamnetin (80 μ g/mL) significantly inhibited the mRNA expression of proinflammatory factors including TLR-2 (A), TLR-4 (B), Dectin-1 (C), IL-1 β (D), TNF- α (E) in HCECs, and TLR-2 (F), TLR-4 (G), Dectin-1 (H), IL-1 β (I), TNF- α (J) in RAW264.7 cells. All data were mean \pm SEM and analyzed using an unpaired, two-tailed Student's *t*-test.

infiltration, and airway remodeling were remarkably attenuated by isorhamnetin in mice. Moreover, according to H&E staining, corneal stroma with isorhamnetin treatment had more regularly arranged collagen fiber and less infiltrated inflammatory cells. Therefore we conclude that isorhamnetin effectively reduces neutrophil recruitment and ameliorates corneal damage.

Previous studies suggested that isorhamnetin has protective effects in various inflammatory diseases, such as acute lung injury and hepatitis.⁷ Yang et al.⁴⁹ proved that isorhamnetin treatment not only can significantly reduce the level of inflammatory cytokines in bronchoalveolar lavage fluid of mice, but also can protect mice from LPS-induced acute lung injury through inhibiting the activation of

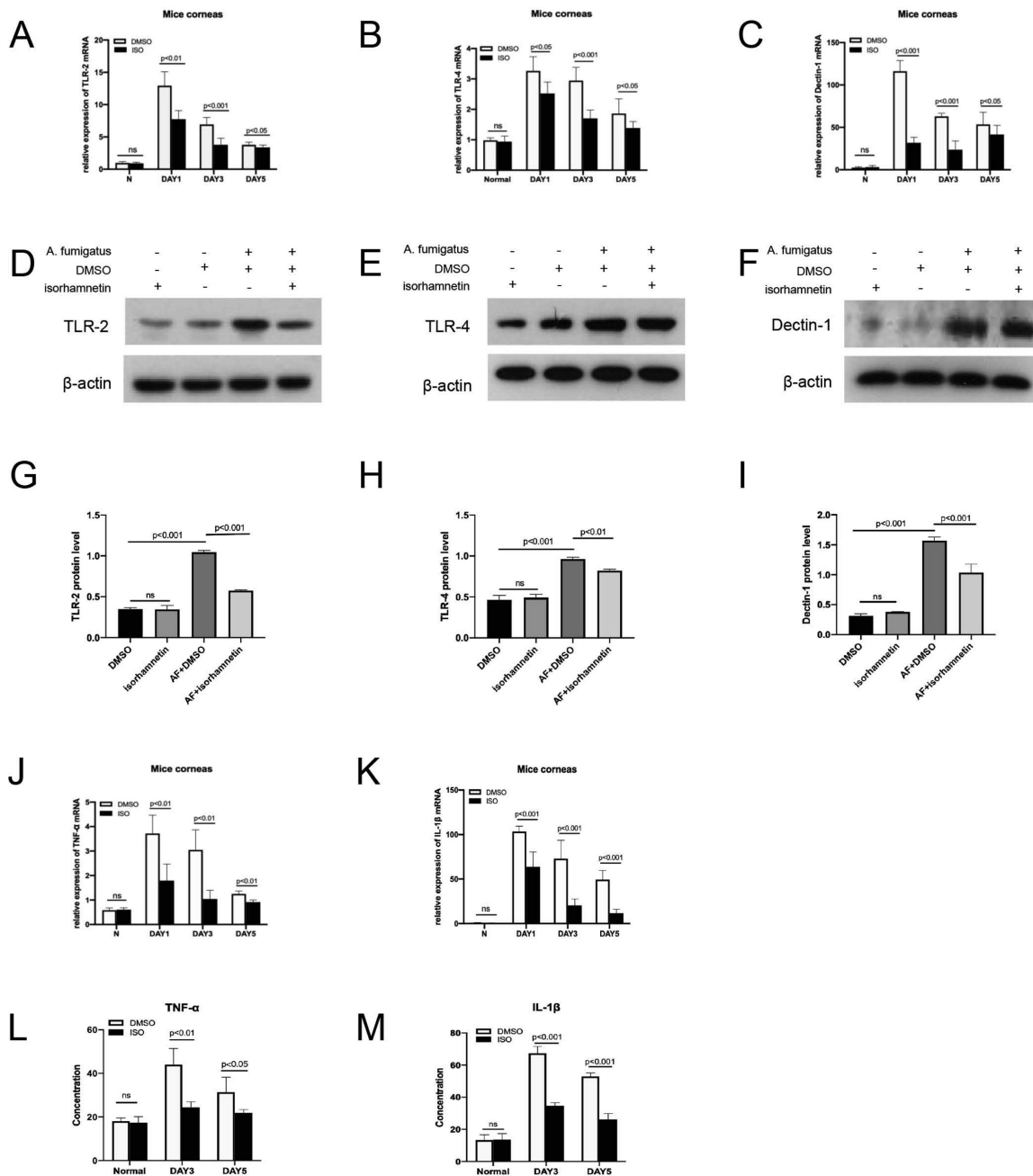


FIGURE 6. Effects of isorhamnetin on the inflammatory response in *A. fumigatus* infected mouse cornea. qRT-PCR results for TLR-2 (A), TLR-4 (B), Dectin-1 (C) TNF- α (J) and IL-1 β (K) at 1,3, and 5 days p. i. Western blot results and grayscale analysis of TLR-2 (D, G), TLR-4 (E, H), Dectin-1 (F, I) at 3 days p. i. ELISA results of TNF- α (L) and IL-1 β (M) at 3 and 5 days p. i. (n = 6 mice/group). All data were mean \pm SEM and analyzed by an unpaired, two-tailed Student's *t*-test.

cyclooxygenase-2. Moreover, a recent study⁵⁰ revealed that isorhamnetin directly interacts with TLR4/MD-2 complex to prevent TLR4-mediated inflammatory cascade, which is consistent with the study by Kim et al.²¹ that isorhamnetin suppressed LPS induced inflammation in mouse microglia by inactivating NF- κ B and blocking TLR4 pathway, reducing the expression of inflammatory factors such as TNF- α and IL-1 β . In this study, we detected the expression of PRRs including TLR-2, TLR-4 and Dectin-1, and downstream inflammatory factors TNF- α and IL-1 β in vitro and in vivo. Our results demonstrated that isorhamnetin has the inhibitory effect

on both PRRs and inflammatory factors in *A. fumigatus*-infected HCECs and mice with FK.

In the FK innate immunity, PRRs such as TLRs and CLRs recognize and bind to fungal pathogen-related molecular patterns (e.g. β -1,3 glucan), which in turn recruits transduction adaptor MyD88 to activate transcription factor NF- κ B and mitogen-activated protein kinases, mediating induction of inflammatory cytokine gene expression.⁵¹ In addition, Dectin-1, one of the most potent CLRs, promotes cytokine release through Dectin-1/Raf-1 signal pathway and interacts with TLR-2 to induce the production of chemokines

CXCL1 and CXCL8, recruiting phagocytes to clear fungi.^{52,53} TNF- α and IL-1 β are produced by phagocytes, mediating the recruitment, activation and adherence of leukocytes that release oxidants and proteolytic enzymes to remove pathogens.⁵⁴ As a result, a huge amount of toxic substances generated by the inflammatory cascade would impair corneal epithelium, damaging corneal stroma structure.^{55,56} Hence, through inhibition of PRRs and proinflammatory factors, isorhamnetin restrained inflammation in mice corneas with FK, which would relieve corneal tissue damage caused by excessive inflammatory response to improve prognosis.

More importantly, there is a complex relationship between fungal growth and corneal inflammation during FK progression. Our previous studies have shown that either the antifungal agents or immunosuppressive treatment could decrease FK clinical scores in mice.^{29,57} Interestingly, the fungal load could be reduced exclusively through inhibiting inflammatory response.^{58,59} For instance, blocking inflammation with suberoylanilide hydroxamic acid, a histone deacetylase inhibitor, could reduce fungal burden in FK mice,⁵⁹ but the underlying mechanism needs to be further studied.

In summary, we conclude that isorhamnetin may improve the outcome of *A. fumigatus* keratitis via three potential mechanisms: inhibiting fungal invasion of cornea, reducing neutrophil recruitment in infected sites, and inhibiting the expression of PRRs and inflammatory factors. Therefore isorhamnetin is a promising compound that has the potential for FK treatment.

Acknowledgments

Supported by the National Natural Science Foundation of China (No.81470609; No.81870632; No.81500695), and the Natural Science Foundation of Shandong Province (No. ZR2019BH004).

Disclosure: **X. Tian**, None; **X. Peng**, None; **J. Lin**, None; **Y. Zhang**, None; **L. Zhan**, None; **J. Yin**, None; **R. Zhang**, None; **G. Zhao**, None

References

- Huang JF, Zhong J, Chen GP, et al. A Hydrogel-Based Hybrid Theranostic Contact Lens for Fungal Keratitis. *ACS Nano*. 2016;10:6464–6473.
- Kredics L, Narendran V, Shobana CS, et al. Filamentous fungal infections of the cornea: a global overview of epidemiology and drug sensitivity. *Mycoses*. 2015;58:243–260.
- Tabatabaei SA, Soleimani M, Tabatabaei SM, et al. The use of in vivo confocal microscopy to track treatment success in fungal keratitis and to differentiate between Fusarium and Aspergillus keratitis. *Int Ophthalmol*. 2020;40:483–449.
- Aveyard J, Deller RC, Lacey R, et al. Antimicrobial Nitric Oxide Releasing Contact Lens Gels for the Treatment of Microbial Keratitis. *ACS Appl Mater Interfaces*. 2019;11:37491–37501.
- Narayana S, Krishnan T, Ramakrishnan S, et al. Mycotic Antimicrobial Localized Injection: A Randomized Clinical Trial Evaluating Intrastromal Injection of Voriconazole. *Ophthalmology*. 2019;126:1084–1089.
- Chirumbolo S. Anti-inflammatory action of isorhamnetin. *Inflammation*. 2014;37:1200–1201.
- Gong G, Guan YY, Zhang ZL, et al. Isorhamnetin: A review of pharmacological effects. *Biomed Pharmacother*. 2020;128:110301.
- Chi G, Zhong W, Liu Y, et al. Isorhamnetin protects mice from lipopolysaccharide-induced acute lung injury via the inhibition of inflammatory responses. *Inflamm Res*. 2016;65:33–41.
- Jnawali H, Jeon D, Jeong M, et al. Antituberculosis Activity of a Naturally Occurring Flavonoid, Isorhamnetin. *J Nat Prod*. 2016;79:961–969.
- Dai W, Bi J, Li F, et al. Antiviral Efficacy of Flavonoids against Enterovirus 71 Infection in Vitro and in Newborn Mice. *Viruses*. 2019;11:v11070625.
- Xu Y, Tang C, Tan S, et al. Cardioprotective effect of isorhamnetin against myocardial ischemia reperfusion (I/R) injury in isolated rat heart through attenuation of apoptosis. *J Cell Mol Med*. 2020;24:6253–6262.
- Ishola I, Osele M, Chijioke M, Adeyemi OJBr. Isorhamnetin enhanced cortico-hippocampal learning and memory capability in mice with scopolamine-induced amnesia: Role of antioxidant defense. *Brain Res*. 2019;1712:188–196.
- Park C, Cha H, Choi E, et al. Isorhamnetin induces cell cycle arrest and apoptosis via reactive oxygen species-mediated AMP-activated protein kinase signaling pathway activation in human bladder cancer cells. *Cancers (Basel)*. 2019;11:1494.
- Wang J, Gong H, Zou H, Liang L, Wu XJMr. Isorhamnetin prevents H2O2-induced oxidative stress in human retinal pigment epithelial cells. *Mol Med Rep*. 2018;17:648–652.
- Chang Z, Wang J, Jing Z, et al. Protective effects of isorhamnetin on pulmonary arterial hypertension: in vivo and in vitro studies. *Phytother Res*. 2020;34:2730–2744.
- Lu X, Liu T, Chen K, et al. Isorhamnetin: A hepatoprotective flavonoid inhibits apoptosis and autophagy via P38/PPAR- α pathway in mice. *Biomed Pharmacother*. 2018;103:800–811.
- Bhattacharya D, Ghosh D, Bhattacharya S, et al. Antibacterial activity of polyphenolic fraction of Kombucha against *Vibrio cholerae*: targeting cell membrane. *Lett Appl Microbiol*. 2018;66:145–152.
- Labeled A, Ferhat M, Labeled-Zouad I, et al. Compounds from the pods of *Astragalus armatus* with antioxidant, anticholinesterase, antibacterial and phagocytic activities. *Pharm Biol*. 2016;54:3026–3032.
- Li J, Wu R, Qin X, et al. Isorhamnetin inhibits IL1 β induced expression of inflammatory mediators in human chondrocytes. *Mol Med Rep*. 2017;16:4253–4258.
- Qi F, Sun JH, Yan JQ, et al. Anti-inflammatory effects of isorhamnetin on LPS-stimulated human gingival fibroblasts by activating Nrf2 signaling pathway. *Microb Pathog*. 2018;120:37–41.
- Kim S, Jin C, Kim C, et al. Isorhamnetin alleviates lipopolysaccharide-induced inflammatory responses in BV2 microglia by inactivating NF- κ B, blocking the TLR4 pathway and reducing ROS generation. *Int J Mol Med*. 2019;43:682–692.
- Berger E. Understanding the Role of Pro-resolving Lipid Mediators in Infectious Keratitis. *Adv Exp Med Biol*. 2019;1161:3–12.
- van de Veerdonk FL, Gresnigt MS, Romani L, et al. *Aspergillus fumigatus* morphology and dynamic host interactions. *Nat Rev Microbiol*. 2017;15:661–674.
- Li C, Zhao G, Che C, et al. The Role of LOX-1 in Innate Immunity to *Aspergillus fumigatus* in Corneal Epithelial Cells. *Invest Ophthalmol Vis Sci*. 2015;56:3593–3603.
- Snarr BD, St-Pierre G, Ralph B, et al. Galectin-3 enhances neutrophil motility and extravasation into the airways during *Aspergillus fumigatus* infection. *PLoS Pathog*. 2020;16:e1008741.
- de Jesus Carrion S, Abbondante S, Clark HL, et al. *Aspergillus fumigatus* corneal infection is regulated by chitin synthases

- and by neutrophil-derived acidic mammalian chitinase. *Eur J Immunol.* 2019;49:918–927.
27. Bernut A, Loynes CA, Floto RA, et al. Deletion of cfr leads to an excessive neutrophilic response and defective tissue repair in a zebrafish model of sterile inflammation. *Front Immunol.* 2020;11:1733.
 28. Fan Y, Li C, Peng X, et al. Perillaldehyde ameliorates *Aspergillus fumigatus* keratitis by activating the Nrf2/HO-1 signaling pathway and inhibiting dectin-1-mediated inflammation. *Invest Ophthalmol Vis Sci.* 2020;61:51.
 29. Zhan L, Peng X, Lin JY, et al. Honokiol reduces fungal load, toll-like receptor-2, and inflammatory cytokines in *Aspergillus fumigatus* keratitis. *Invest Ophthalmol Vis Sci.* 2020;61:48.
 30. Sun Q, Li C, Lin J, et al. Celastrol ameliorates *Aspergillus fumigatus* keratitis via inhibiting LOX-1. *Int Immunopharmacol.* 2019;70:101–109.
 31. Borkovich KA, Zhang Y, Wang C, et al. Control effect and possible mechanism of the natural compound phenazine-1-carboxamide against *Botrytis cinerea*. *Plos One.* 2015;10:e0140380.
 32. Peng XD, Zhao GQ, Lin J, et al. Fungus induces the release of IL-8 in human corneal epithelial cells, via Dectin-1-mediated protein kinase C pathways. *Int J Ophthalmol.* 2015;8:441–447.
 33. Zhou Y, Lin J, Peng X, et al. The role of netrin-1 in the mouse cornea during *Aspergillus fumigatus* infection. *Int Immunopharmacol.* 2019;71:372–381.
 34. Niu Y, Zhao G, Li C, et al. *Aspergillus fumigatus* increased PAR-2 expression and elevated proinflammatory cytokines expression through the pathway of PAR-2/ERK1/2 in cornea. *Invest Ophthalmol Vis Sci.* 2018;59:166–175.
 35. Yin M, Li C, Peng X, et al. *Aspergillus fumigatus* expression and role of calcitonin gene-related peptide in mouse keratitis. *Int J Ophthalmol.* 2019;12:697–704.
 36. Yuan K, Zhao G, Che C, et al. Dectin-1 is essential for IL-1beta production through JNK activation and apoptosis in *Aspergillus fumigatus* keratitis. *Int Immunopharmacol.* 2017;52:168–175.
 37. Li C, Lin J, Zhao G, et al. The role of autophagy in the innate immune response to fungal keratitis caused by *Aspergillus fumigatus* infection. *Invest Ophthalmol Vis Sci.* 2020;61:25.
 38. Cole DC, Govender NP, Chakrabarti A, Sacarlal J, Denning DW. Improvement of fungal disease identification and management: combined health systems and public health approaches. *Lancet Infect Dis.* 2017;17:e412–e419.
 39. Keay LJ, Gower EW, Iovienu A, et al. Clinical and microbiological characteristics of fungal keratitis in the United States, 2001–2007: a multicenter study. *Ophthalmology.* 2011;118:920–926.
 40. Prajna NV, Krishnan T, Rajaraman R, et al. Mycotic ulcer treatment trial, effect of oral voriconazole on fungal keratitis in the Mycotic Ulcer Treatment Trial II (MUTT II): a randomized clinical trial. *JAMA Ophthalmol.* 2016;134:1365–1372.
 41. Ren QC, Li XH, Li QY, et al. Total flavonoids from sea buckthorn ameliorates lipopolysaccharide/cigarette smoke-induced airway inflammation. *Phytother Res.* 2019;33:2102–2117.
 42. Mamatova AS, Korona-Glowniak I, Skalicka-Wozniak K, et al. Phytochemical composition of wormwood (*Artemisia gmelinii*) extracts in respect of their antimicrobial activity. *BMC Complement Altern Med.* 2019;19:288.
 43. Tagousop CN, Tamokou JD, Ekom SE, et al. Antimicrobial activities of flavonoid glycosides from *Graptophyllum grandulosum* and their mechanism of antibacterial action. *BMC Complement Altern Med.* 2018;18:252.
 44. Cespedes CL, Salazar JR, Ariza-Castolo A, et al. Biopesticides from plants: *Calceolaria integrifolia* s.l. *Environ Res.* 2014;132:391–406.
 45. Plato A, Willment JA, Brown GD. C-type lectin-like receptors of the dectin-1 cluster: ligands and signaling pathways. *Int Rev Immunol.* 2013;32:134–156.
 46. Brown GD. Dectin-1: a signalling non-TLR pattern-recognition receptor. *Nat Rev Immunol.* 2005;6:33–43.
 47. Sun Y, Abbondante S, Karmakar M, et al. Neutrophil caspase-11 is required for cleavage of caspase-1 and secretion of IL-1beta in *Aspergillus fumigatus* infection. *J Immunol.* 2018;201:2767–2775.
 48. Drummond RA, Brown GD. The role of Dectin-1 in the host defense against fungal infections. *Curr Opin Microbiol.* 2011;14:392–399.
 49. Yang B, Li XP, Ni YF, et al. Protective effect of isorhamnetin on lipopolysaccharide-induced acute lung injury in mice. *Inflammation.* 2016;39:129–137.
 50. Chauhan AK, Kim J, Lee Y, Balasubramanian PK, Kim Y. Isorhamnetin has potential for the treatment of *Escherichia coli*-induced sepsis. *Molecules.* 2019;24:3984.
 51. Pearlman E, Sun Y, Roy S, et al. Host defense at the ocular surface. *Int Rev Immunol.* 2013;32:4–18.
 52. Zhao GQ, Lin J, Hu LT, et al. The role of Dectin-1/Raf-1 signal cascade in innate immune of human corneal epithelial cells against *Aspergillus fumigatus* infection. *Int J Ophthalmol.* 2016;9:1371–1375.
 53. Zhao G, Xue Y, Lin J, et al. Co-regulation of Dectin-1 and TLR2 in inflammatory response of human corneal epithelial cells induced by *Aspergillus fumigates*. *Int J Ophthalmol.* 2016;9:185–190.
 54. Kawai T, Akira S. The role of pattern-recognition receptors in innate immunity: update on Toll-like receptors. *Nat Immunol.* 2010;11:373–384.
 55. Gao X, Zhao G, Li C, et al. LOX-1 and TLR4 affect each other and regulate the generation of ROS in *A. fumigatus* keratitis. *Int Immunopharmacol.* 2016;40:392–399.
 56. Guo H, Gao J, Wu X. Toll-like receptor 2 siRNA suppresses corneal inflammation and attenuates *Aspergillus fumigatus* keratitis in rats. *Immunol Cell Biol.* 2012;90:352–357.
 57. Gu L, Lin J, Wang Q, et al. Dimethyl itaconate protects against fungal keratitis by activating the Nrf2/HO-1 signaling pathway. *Immunol Cell Biol.* 2020;98:229–241.
 58. Gao N, Kumar A, Yu FS. Matrix metalloproteinase-13 as a target for suppressing corneal ulceration caused by *Pseudomonas aeruginosa* infection. *J Infect Dis.* 2015;212:116–127.
 59. Li X, Yuan M, Yin R, et al. Histone deacetylase inhibitor attenuates experimental fungal keratitis in mice. *Sci Rep.* 2019;9:9859.